NASA Technical Paper 1057

Effect of Coolant Flow Ejection on Aerodynamic Performance of Low-Aspect-Ratio Vanes

II - Performance With Coolant Flow Ejection at Temperature Ratios up to 2

Jeffrey E. Haas and Milton G. Kofskey

OCTOBER 1977

NASA

NASA Technical Paper 1057

Effect of Coolant Flow Ejection on Aerodynamic Performance of Low-Aspect-Ratio Vanes

II - Performance With Coolant Flow Ejection at Temperature Ratios up to 2

Jeffrey E. Haas
Propulsion Laboratory
U.S. Army R&T Laboratories (AVRADCOM)
and
Milton G. Kofskey
Lewis Research Center
Cleveland, Ohio

National Aeronautics
and Space Administration

Scientific and Technical Information Office

1977

EFFECT OF COOLANT FLOW EJECTION ON AERODYNAMIC PERFORMANCE OF LOW-ASPECT-RATIO VANES II - PERFORMANCE WITH COOLANT FLOW EJECTION AT TEMPERATURE RATIOS UP TO 2

by Jeffrey E. Haas and Milton G. Kofskey

Lewis Research Center and
U. S. Army Air Mobility R&D Laboratory

SUMMARY

The aerodynamic performance of a 0.5 aspect ratio turbine vane configuration with coolant flow ejection was experimentally determined in a full-annular cascade. The vanes were tested at a nominal mean-section ideal critical velocity ratio of 0.890 over ranges of primary-to-coolant total temperature ratio from 1.0 to 2.08 and coolant-to-primary total pressure ratio from 1.0 to 1.4. This corresponded to coolant flows from 3.0 to 10.7 percent of the primary flow. To obtain these ranges of total pressure and total temperature ratio, dry pressurized air at a pressure of 8.3 newtons per square centimeter and a temperature between 295 and 405 K was used for the primary flow, and gaseous nitrogen at a pressure between 8.3 and 11.6 newtons per square centimeter and a temperature between 195 and 295 K was used as vane coolant.

The overall thermodynamic efficiency increased with decreasing coolant-to-primary-total pressure ratio and increasing primary-to-coolant total temperature ratio. At a coolant temperature and pressure ratio of 1.0, the percentage decrease in thermodynamic efficiency per percent coolant flow was 1.07. In addition, a total pressure ratio contour plot at the vane exit survey plane showed that the ejection of coolant flow caused a considerably thicker and shallower wake compared to the plugged vane configuration. Larger loss regions near the endwalls, particularly near the hub, were also noted with the coolant flow ejection.

A comparison of the results from the subject investigation with those from a reference investigation having vanes with an aspect ratio of about 1.2 showed that between a coolant-to-primary total pressure ratio of 1.0 and about 1.15, the efficiency for the subject vanes was lower and the penalty associated with the coolant flow was larger than that for the reference vanes. At a coolant temperature and pressure ratio of 1.0, the percentage decrease in thermodynamic efficiency per percent coolant flow was 0.57 for the reference configuration.

INTRODUCTION

Advanced small turboshaft engines in the 1.00- to 4.50-kilogram-per-second, 250- to 1100-kilowatt class are being designed to operate at cycle pressure ratios of 10 to 1 or higher, with turbine inlet temperatures as high as 1550 K. The high compressor pressure ratio, together with the small mass flow, results in a turbine design with a small annulus area and, therefore, a small blade height. A high turbine inlet temperature requires the use of vane and blade cooling air, and therefore, the stator and rotor blade profiles must be fabricated longer and thicker than desired from an aerodynamic standpoint to provide adequate space for cooling passages. Long chord lengths and small blade heights result in a low aspect ratio design.

Reference 1 indicates that low aspect ratio designs have significantly greater secondary flow losses than high aspect ratio designs because the secondary flow fields encompass a significantly greater proportion of the airflow channel. Reference 2 showed experimentally that low momentum fluids on the blade surfaces and endwalls and in the blade wakes can be transported radially and circumferentially to form regions of high losses. Blade cooling can compound this problem because low momentum coolant flow being ejected from holes and slots can cause increased boundary layer losses and can also be transported into the secondary loss regions to further increase the total loss.

To study the effect on performance of coolant flow ejection from the surfaces of a small turbine vane, an experimental investigation was conducted using the GE-12 first-stage gas generator turbine vanes. These vanes had a height of 1.75 centimeters and an aspect ratio of about 0.5. Performance measurements were made in a full-annular cascade and consisted of vane exit radial and circumferential surveys of flow angle, total pressure, and total temperature.

In order to establish a basis for evaluating the effect on performance of coolant flow ejection, the performance of the solid vanes was first determined. For these tests the coolant holes were plugged flush with the vane surfaces to prevent internal flow circulation and surface flow disturbances. Reference 3 describes these performance tests and results. These baseline tests were conducted over a range of mean-section ideal critical velocity ratio from 0.64 to 0.98. Ideal critical velocity ratio was calculated from the vane inlet total to vane exit aftermixed static pressure ratio at the mean section. At the design value of mean-section ideal critical velocity ratio (0.894), the overall vane aftermixed efficiency was determined to be 0.929.

This report describes the performance of the vanes with coolant ejection. Annular surveys were made downstream of the vane trailing edge at a nominal value of mean-section ideal critical velocity ratio of 0.890. Aerodynamic performance data were obtained over a range of primary-to-coolant total temperature ratio from 1.0 to 2.08 and a range of coolant-to-primary total pressure ratio from 1.0 to 1.4. This resulted in a range of coolant flows from 3.0 to 10.7 percent of the primary flow. To obtain a range

of total temperature ratio, dry pressurized air at a temperature between 295 and 405 K was used for the primary flow, and gaseous nitrogen at a temperature between 195 and 295 K was used as vane coolant.

Presented in this report for various coolant flow rates are experimentally determined overall vane aerodynamic efficiencies, radial variations in vane primary and thermodynamic efficiency, pressure ratio and flow angle, and radial and circumferential variations in vane exit total pressure. In addition, the experimentally obtained coolant flow rates and aftermixed efficiencies are compared to those obtained using the prediction method of reference 4. Finally, to provide a comparison of the primary and thermodynamic efficiencies obtained with cooled vane configurations having different aspect ratios, the experimental results from the subject investigation are compared to the results from a reference investigation.

SYMBOLS

$\overline{\overline{m}}$ total mass flow per passage, kg/sec

p pressure, N/cm^2

R gas constant, J/(kg)(K)

r radial direction, m

T temperature, K

V velocity, m/sec

y ratio of coolant flow to primary flow

y_c ratio of coolant flow to total flow

y_p ratio of primary flow to total flow

α flow angle measured from axial direction, deg

γ ratio of specific heats

η efficiency at radius r based on kinetic energy

$\overline{\overline{\eta}}$ overall efficiency based on kinetic energy

Θ vane angular spacing, deg

θ circumferential direction, deg

ρ density, kg/m^3

Subscripts:

c coolant flow

cr	flow conditions at Mach 1
h	hub
i	survey position closest to inner (hub) wall
id	ideal or isentropic
k	survey position closest to outer (tip) wall
P	primary
p	primary flow
T	thermodynamic
t	tip
u	tangential direction
z	axial direction
0	zero coolant flow (solid or plugged configuration)
1	station at vane inlet (fig. 5)
2	station downstream of vane trailing edge where survey measurements were taken (fig. 5)
3	station downstream of vane trailing edge where static pressures were measured (fig. 5)
3M	station downstream of vane trailing edge where flow is assumed to be circumferentially mixed (uniform) (fig. 5)

Superscript:

'	total-state condition

APPARATUS

The full-annular cascade facility consisted primarily of the test section, the inlet and exhaust piping, the coolant supply lines and the control valves. A photograph and a cross-sectional view of the facility are shown in figures 1 and 2, respectively. Dry pressurized air at a temperature between 295 and 405 K flowed through the inlet section, test blading, and then was exhausted into the central exhaust system. Gaseous nitrogen at a temperature between 195 and 295 K was used as vane coolant and was routed to the vane hub and tip as shown in figures 1 and 2. Control valves at the cascade inlet and exit were used to control the flow conditions upstream and downstream of the test section.

The inlet, consisting of a bellmouth and a short inlet section, provided uniform inlet conditions with a small boundary layer growth at the vane inlet.

The 24 vane test section was a full-annular ring consisting of 12 segments which had two vanes per segment. A photograph of two segments is shown in figure 3. These test vanes were the first-stage gas generator turbine vanes from the GE-12 demonstrator engine. The vanes were slightly twisted and had a height of 1.75 centimeters and an axial chord of 2.12 centimeters. The vane aspect ratio and solidity (both based on actual chord length) were about 0.5 and 1.5, respectively. The stator hub to tip radius ratio was about 0.8, and the mean-radius was about 8.7 centimeters. The vane design velocity diagrams are shown in figure 4.

In this investigation, the coolant was ejected from the surfaces of all 24 vanes as shown in the insert in figure 3. The coolant routed through the vane tip was ejected from the pressure surface film cooling holes and trailing edge holes, while the coolant routed through the vane hub was ejected from the double row of film cooling holes on the suction surface. Both the vane hub and tip coolant entered the test section through separate plenum chambers. From these plenum chambers the coolant was distributed as evenly as possible around the full circumference of the test section and flowed into the vanes through holes in the vane platforms.

INSTRUMENTATION

Figure 5 shows station nomenclature and the instrumentation used to measure wall static pressure, total temperature, total pressure, and flow angle. Instrumentation at the vane inlet (station 1) measured static pressure and total temperature. Static pressures were obtained from eight taps with four on the inner wall and four on the outer wall of the annulus. The inner and outer taps were located opposite each other at 90° intervals around the circumference at a distance approximately 1.60 centimeters upstream of the vanes. The temperature was measured with three thermocouple rakes, each containing three thermocouples.

Vane performance was based on measurements obtained from two survey probes located 0.27 centimeter downstream of the vane trailing edge. An angle probe (fig. 6) located at station 2 (fig. 5) was used first to determine the variation in flow angle both radially and circumferentially. The angle probe consisted of two parallel tubes with the sensing end cut off to form a 60° wedge. Stainless-steel tubing with an outside diameter of 0.038 centimeter and a wall thickness of 0.006 centimeter was used. Calibration of this probe showed no sensitivity to Mach number effects up to 0.9.

After the angle survey was made, a total pressure total temperature probe (fig. 7) was installed and positioned at a fixed angle of 77.2° from the axial direction. This angle was an arithmetrical mean of that measured by the angle probe. This angle was

subsequently found to be with 0.25° of the mass-averaged value. The variation in total pressure loss was measured using a differential pressure transducer referenced to the vane inlet static pressure. A copper-constantan thermocouple was used to measure the total temperature. The total pressure sensing tube was stainless-steel tubing with an outside diameter of 0.038 centimeter and a wall thickness of 0.006 centimeter. The sensing end of the tube had an inside bevel of 30° to reduce the sensitivity to deviations in actual flow angle from the average setting. Calibration of this probe showed total pressure measurements were insensitive to deviations in flow angle of ±10° and Mach number effects up to 0.9. Angle surveys indicated that the maximum deviation in flow angle was only ±5° in both the radial and circumferential direction from the fixed setting angle. The probe support (fig. 7) was inclined approximately 25° from the axial direction to obtain measurements near the hub wall. Measurements near the outer wall could also be obtained with this probe because the combined effects of slot width and probe setting angle of 77.2° allowed the probe tip to be withdrawn all the way to this location.

Circumferentially, the surveys were arbitrarily limited to one blade spacing (15°) as shown in figure 5. The survey area at station 2 (fig. 5) was distorted because the probe sensing point was displaced from the probe stem. This occurred even though the probe system covered a true segment of the annulus.

At station 3, located approximately 0.89 centimeter downstream of the vane trailing edge, 24 static taps (12 each on the inner and outer walls) were spaced at various circumferential positions in order to determine the static pressure variation across the passage. These static taps were installed in several passages because the physical size of the tubing prohibited installation in only one passage. In figure 5 they are shown in the test channel to illustrate their collective relative positions.

The coolant flow rate in the vane hub and tip supply lines was measured using separate calibrated venturi meters. The static pressure and total temperature of the coolant were measured prior to entry into the vanes.

PROCEDURE

Dry pressurized air controlled to a pressure of about 8.3 newtons per square centimeter and at a total temperature between 295 and 405 K was supplied through control valves. From the cascade the flow was piped into the exhaust system. The exit test conditions were set by controlling the pressure at the vane exit with a throttle valve located in the exhaust system. A tip static tap located downstream of the test section was used to set the pressure ratio.

The vane coolant was supplied through the separate vane hub and tip supply lines at a pressure between about 8.3 and 11.6 newtons per square centimeter and at a total temperature between 195 and 295 K. This resulted in ranges of primary-to-coolant total

temperature ratio from 1.0 to 2.08 and coolant-to-primary total pressure ratio from 1.0 to 1.4. The coolant pressures and temperatures were maintained equal in both supply lines at all times. The desired coolant temperature was obtained by using a heat exchanger located upstream of the venturi runs.

All of the tests in this investigation were conducted at a nominal mean-section ideal critical velocity ratio of 0.890. This ideal critical velocity ratio was calculated from the vane inlet total to vane exit aftermixed static pressure ratio at the mean section. At a given primary-to-coolant total temperature ratio and total pressure ratio, data were obtained at 11 different radii over the vane height. At each fixed radius, the probe was moved circumferentially to cover approximately the vane spacing (15°) with data being obtained at discrete points approximately every 1°. At each discrete point the probe movement was stopped and the probe temperature and pressure were allowed to reach equilibrium before taking the data point. The output signals of the thermocouples and pressure transducers were digitized and recorded on magnetic tape.

DATA REDUCTION

The cooled vane performance presented herein was calculated from probe position, the probe survey measurement of total pressure and total temperature and wall static pressures. In addition, the following assumptions were used for data reduction purposes:

(1) The static pressure variation at station 3 is equal to the static pressure variation at station 2 since there is no change in the annulus area between these two stations.

(2) The static pressure at station 3 varies linearly with radius. The hub and tip wall static pressures, at station 3, were used to linearly interpolate this variation in pressure.

(3) The exit flow angle (station 2) is constant circumferentially and radially. The design value of 77.2° was used for the performance data presented herein.

The calculation of the vane efficiencies was based on the determination of a hypothetical state where it was assumed that the flow has mixed to a circumferentially uniform condition. The application of the conservation equations to an annular-sector control volume to obtain this aftermixed state, at each radius, was described fully in reference 5. The aftermixed vane efficiency is used herein because it is theoretically independent of the axial location of the survey measurement plane. It should be noted that the aftermixed efficiency contains not only the vane profile and end wall losses, but also the mixing loss.

For cooled vane performance, both the thermodynamic and primary efficiencies are in general use. Primary efficiency is defined as the ratio of the actual aftermixed kinetic energy to the ideal aftermixed kinetic energy of the primary flow only. The ther-

modynamic efficiencies at a given radius $\bar{\eta}_{3M,\,T}(r)$ and for the total passage $\bar{\bar{\eta}}_{3M,\,T}$ are given by reference 5

$$\bar{\eta}_{3M,\,T}(r) = \frac{V_{3M}^2(r)}{y_p(r)\left[V_{3M,\,id}^2(r)\right]_p + y_c(r)\left[V_{3M,\,id}^2(r)\right]_c} \tag{1}$$

$$\bar{\bar{\eta}}_{3M,\,T} = \frac{\int_{r_i}^{r_k}\left[\rho_{3M}(r)V_{3M,\,z}(r)V_{3M}^2(r)\right] r\,dr}{\int_{r_j}^{r_k}\rho_{3M}(r)V_{3M,\,z}(r)\left\{y_p(r)\left[V_{3M,\,id}^2(r)\right]_p + y_c(r)\left[V_{3M,\,id}^2(r)\right]_c\right\} r\,dr} \tag{2}$$

where the ideal velocities of the primary $\left[V_{3M,\,id}(r)\right]_p$ and coolant flows $\left[V_{3M,\,id}(r)\right]_c$ are given by

$$\left[V_{3M,\,id}(r)\right]_p = \sqrt{\frac{2\gamma}{\gamma - 1}RT_1'\left\{1 - \left[\frac{P_{3M}(r)}{p_1'}\right]^{(\gamma-1)/\gamma}\right\}} \tag{3}$$

$$\left[V_{3M,\,id}(r)\right]_c = \sqrt{\frac{2\gamma}{\gamma - 1}RT_c'\left\{1 - \left[\frac{p_{3M}(r)}{p_c'}\right]^{(\gamma-1)/\gamma}\right\}} \tag{4}$$

The fraction of coolant flow to total flow $y_c(r)$ is assumed to be independent of radius r and to equal

$$y_c = \frac{\bar{\bar{m}}_c}{\bar{\bar{m}}} = 1 - y_p = \text{Constant} \tag{5}$$

(for a given survey) where $\bar{\bar{m}}_c$ is the measured coolant flow rate per passage and $\bar{\bar{m}}$ is the total flow rate per passage given by

$$\bar{\bar{m}} = \int_{r_h}^{r_t}\int_0^{\Theta}\rho_3(r,\Theta)V_{3,\,z}(r,\Theta)r\,d\Theta\,dr \tag{6}$$

The primary efficiencies at a given radius $\bar{\eta}_{3M,\,P}(r)$ and for the total passage $\bar{\bar{\eta}}_{3M,\,P}$ are given by

$$\bar{\eta}_{3M,\,P}(r) = \frac{V_{3M}^2(r)}{y_p\left[V_{3M,\,id}^2(r)\right]_p} \tag{7}$$

$$\bar{\bar{\eta}}_{3M,\,P} = \frac{\int_{r_i}^{r_k}\left[\rho_{3M}(r)V_{3M,\,z}(r)V_{3M}^2(r)\right]r\,dr}{\int_{r_i}^{r_k}\left\{y_p\rho_{3M}(r)V_{3M,\,z}(r)\left[V_{3M,\,id}^2(r)\right]_p\right\}r\,dr} \tag{8}$$

RESULTS AND DISCUSSION

Presented in this section are the experimentally determined overall vane aerodynamic efficiencies, radial variations in vane efficiency, pressure ratio, and flow angle, and radial and circumferential variations in vane exit total pressure for various coolant flow rates. Comparisons are made between the cooled vane configuration and the plugged vane configuration of reference 3. In addition, the measured coolant mass flow rates and the calculated aftermixed efficiencies are compared to those obtained using the prediction method of reference 4. Finally, to provide a comparison of the efficiencies obtained with cooled vane configurations having different aspect ratios, the experimental results from the subject investigation are compared to the results from a reference investigation.

Flow Discharge Angle

At each radial position the flow angle was averaged over the vane spacing. The maximum angle deviation was only $\pm 5^{\circ}$ in the circumferential direction. Figure 8 shows the radial variation in the flow discharge angle. There was only a small variation in the radial angle distribution for 3 and 10 percent coolant flow ejection. The average flow angle was about 4° higher than for the plugged vane configuration (ref. 3). The arithmetically averaged flow angle for both configurations was found to be within 0.5° of the respective mass-averaged values. Based on previous investigations (refs. 6

and 7), which showed the flow angle to be relatively insensitive to coolant ejection, it was believed that most of this difference was due to something other than the coolant flow ejection. One hypothesis for this difference is shown in figure 9. This figure shows the approximate mean camber angles at the trailing edge for the plugged and cooled vane configurations. For these GE-12 vanes the trailing edge coolant ejection was from the pressure surface, instead of from a slot in the trailing edge. As shown in figure 9(a), for the plugged vane tests the filler material was contoured to form a continuous pressure surface. This resulted in a trailing edge mean camber angle of about 72° (based on the average angle from the axial direction formed by the suction and pressure surfaces). However, for the tests with coolant flow ejection (fig. 9(b)), the trailing edge mean camber angle was about 76°. Thus, there was a 4° difference in the mean camber angles between the cooled and plugged vane configurations which could have caused the 4° difference in the measured flow discharge angle. The 4° difference in the average flow angle between the plugged and cooled vane configurations was expected to have a negligible effect on the measured total pressure since the total pressure probe was insensitive to deviations in flow angle of $\pm 10^{\circ}$.

Variation of Coolant Flow

Figure 10 shows the variation of coolant mass flow fraction with pressure and temperature ratio. This figure indicates that the coolant mass flow fraction increased with both temperature ratio and pressure ratio. The increase in coolant mass flow fraction with an increase in temperature ratio was due to a decrease in the primary mass flow as the temperature of the primary flow increased and an increase in the coolant mass flow as the temperature of the coolant flow decreased. The increase in coolant mass flow fraction with pressure ratio was also due to an increase in the ρV of the coolant flow as the pressure of the coolant increased. In this investigation the coolant mass flow covered a range from 3.0 to 10.7 percent of the primary flow.

Variation of Flow Conditions at Vane Exit

Figure 11 shows the blade-to-blade midspan variation of total pressure, static pressure and total temperature at the vane exit survey plane. As expected, at primary-to-coolant temperature ratios greater than one, there were total temperature wakes as well as total pressure wakes. The depth and width of the total pressure wakes remained essentially constant with increasing coolant mass flow fraction. The size of the temperature wakes increased with both pressure and temperature ratio. These temperature

wakes resulted in lower velocities, and thus caused a slight additional loss in vane efficiency.

Overall Aftermixed Efficiency

The overall primary and thermodynamic efficiencies are presented in figure 12 as functions of coolant mass flow fraction and primary-to-coolant total temperature and total pressure ratio. The primary efficiency increased with increasing pressure ratio and decreasing temperature ratio. As shown in equation (7) in the section Data Reduction the primary efficiency reflects the kinetic energy of the mixed primary and coolant flow per unit of primary flow. Figure 12 shows that at a constant temperature ratio, the percentage increase in primary efficiency with pressure ratio was less than the percentage increase in coolant flow. To have the primary efficiency increase with pressure ratio while at the same time have the percentage increase in primary efficiency be less than the percentage increase in coolant mass flow fraction indicates that the numerator of equation (7) decreased as the pressure ratio increased.

The change in primary efficiency with primary-to-coolant total temperature ratio was apparently due to the difference in the kinetic energy of the coolant relative to the primary flow. The kinetic energy of the coolant relative to the primary flow was highest at a temperature ratio of one and increased with coolant-to-primary total pressure ratio. At temperature ratios greater than one, the kinetic energy of the coolant decreased relative to the kinetic energy of the primary flow at all of the coolant to primary total pressure ratios investigated. Therefore, the kinetic energy of the mixed flow increased with decreasing temperature ratio, which in turn caused an increase in primary efficiency.

Figure 12 also shows that the trend in thermodynamic efficiency was opposite to the trend in primary efficiency, that is, the thermodynamic efficiency increased with decreasing pressure ratio and increasing temperature ratio. For a given coolant-to-primary total pressure ratio, the highest thermodynamic efficiencies occurred at the highest primary-to-coolant total temperature ratio or where the kinetic energy of the coolant was lowest relative to the kinetic energy of the primary flow. This was opposite to the trend in primary efficiency because the thermodynamic efficiency is based on the ideal energy of both the primary and the coolant flows. To obtain an increase in thermodynamic efficiency with temperature ratio, the percentage decrease in the actual kinetic energy of the mixed flow was less than the percentage decrease in the ideal kinetic energy of the mixed flow.

Total Pressure Ratio Contour Plots

A contour plot of total pressure ratio is shown in figure 13(a) for a coolant-to-primary total pressure ratio of 1.4 and a primary-to-coolant total temperature ratio of 1.98. This case had the highest amount of coolant flow of all the cases tested. The coolant flow fraction was 10.7 percent. A contour plot for the plugged vane configuration is shown in figure 13(b). This was taken from reference 3.

Comparison of the loss patterns with coolant flow (fig. 13(a)) with the plugged vane configuration (fig. 13(b)) shows that the major difference is the considerably thicker and shallower wake obtained with the coolant flow. As discussed in reference 8 the shallower wake may have been due to the effect of the coolant flow that was ejected from the pressure surface trailing edge holes. The thicker wake, on the other hand, may have been caused by the coolant flow that was ejected from the film cooling holes on the suction and pressure surfaces. The lack of a passage vortex for both configurations suggests that any cross-channel flow of low momentum fluid along the outer wall flowed into the wake without the formation of a passage vortex. Low momentum fluid, which flowed radially inward in the wake may have contributed to the loss region near the hub.

Radial Variation of Aftermixed Efficiency

Figures 14 and 15 show the radial variations in the aftermixed primary and thermodynamic efficiencies, respectively. In both figures the data is plotted to compare the different temperature ratio cases at a constant pressure ratio. Also shown in figures 14 and 15 is the radial variation in efficiency for the plugged vane configuration. The biggest difference between the results for the plugged and cooled vane configurations appears to be in the efficiency near the hub endwall. With coolant flow ejection the efficiency near the hub is much lower than for the plugged vane configuration. Since the slope in efficiency is quite severe near the hub, this much lower level of efficiency with coolant flow ejection might have been attributed to the accuracy in setting the radial position closest to the hub.

Radial Variation of Aftermixed Total Pressure Ratio

Figure 16 shows the radial variation in the aftermixed total pressure ratio. As with figures 14 and 15, the data is plotted to compare the different temperature ratio cases at a constant pressure ratio. The aftermixed total pressure ratio variation for the plugged vane configuration is also shown. As with the radial variation in efficiency, the biggest difference between the plugged and cooled vane configurations occurred near the hub. At

a constant pressure ratio there was only a slight difference in the total pressure between the various temperature ratio cases.

Prediction of Cooled Vane Performance

A prediction method (ref. 4) was developed at the NASA Lewis Research Center to calculate the cooled turbine aerodynamic performance from reduced primary-to-coolant total temperature ratio results. The basic assumption used in this prediction model is that the aerodynamic losses (total-pressure losses) due to boundary layer growth and mixing are assumed to be constant between the actual engine total temperature ratio and the reduced total temperature ratio conditions if the coolant-to-primary momentum ratio is maintained the same. Maintaining the coolant-to-primary momentum ratio constant is equivalent to maintaining the coolant-to-primary total pressure ratio constant. In addition, it is assumed that the total-pressure change due to mixing streams of different total temperatures is negligible in comparison with the total pressure loss due to viscous effects. The validity of this basic assumption was confirmed for the subject vane configuration from the results shown in figure 16. This figure showed that for a constant pressure ratio, the difference in the aftermixed total pressure for the various temperature ratio cases was small.

Figures 17 and 18 show the results of this prediction method as applied to the vane configuration from the subject investigation. Figure 17 shows the predicted coolant flow fractions for various total temperature and total pressure ratios. Figure 18 shows the variations in primary and thermodynamic efficiency for various temperature and pressure ratios. In both figures the experimental results obtained at a total temperature ratio of one were used as the reference case.

Figures 17 and 18 show that, in general, there was good agreement between the predicted and experimental results. The largest difference was in the calculated coolant fraction at a pressure ratio of 1.2 (fig. 17). This, in turn, caused a difference between the calculated and measured primary efficiencies (fig. 18).

Comparison of Cooled Vane Performance Between Different Aspect Ratio Vane Configurations

To provide a comparison of the efficiencies obtained with cooled vane configurations having different aspect ratios, the experimental results from the subject investigation were compared to the results obtained from the investigation of reference 9. The vanes used in this reference investigation had a height of 9.78 centimeters and an aspect ratio of about 1.2. This compared to a vane height of 1.75 centimeters and an aspect ratio of

about 0.5 for the subject vanes. The reference 9 vanes had coolant ejected from a split trailing edge and also from film cooling slots in both the suction and pressure surfaces near the trailing edge. In this reference investigation the vanes were tested over ranges of coolant-to-primary pressure ratio and primary-to-coolant temperature ratio in a four-vane annular-sector cascade.

Figure 19 compares the two configurations in terms of changes in primary and thermodynamic efficiency from the solid (plugged) efficiency per percent coolant flow as a function of coolant-to-primary total pressure ratio for two values of primary-to-coolant total temperature ratio. The percentage decrease in thermodynamic efficiency per percent coolant flow at a coolant temperature and pressure ratio of 1.0 was 1.07 for the subject configuration and 0.57 for the reference 9 configuration.

Figure 19 shows that, between a coolant-to-primary total pressure ratio of 1.0 and about 1.15, the percent change in primary efficiency for the subject vanes is smaller than that for the reference 9 vanes and the percent change in thermodynamic efficiency is greater than that for the reference 9 vanes. This range of coolant-to-primary total pressure ratio is significant, since for engines operating with turbine coolant supplied by compressor bleed, the total pressure ratio for the coolant being supplied to the first-stage turbine vanes is close to 1. It should also be noted that the solid (plugged) vane efficiency for the reference 9 vanes was 0.954 as compared to 0.929 for the subject vanes. Thus, in the range of coolant-to-primary total pressure ratio between 1.0 and about 1.15, the efficiency for the subject vanes was lower and the penalty associated with the coolant flow was larger than that for the reference 9 vanes.

Figure 19 also shows that above a pressure ratio of about 1.15, the penalty associated with the coolant flow was less for the subject vanes. The reason for this reversal in trend is uncertain.

SUMMARY OF RESULTS

The aerodynamic performance of a 0.5 aspect ratio turbine vane configuration with coolant flow ejection was experimentally determined in a full-annular cascade. The vanes were tested at a nominal mean-section ideal critical velocity ratio of 0.890 over ranges of primary-to-coolant total temperature ratio from 1.0 to 2.08 and coolant-to-primary total pressure ratio from 1.0 to 1.4. This corresponded to coolant flows from 3.0 to 10.7 percent of the primary flow. To obtain ranges of total pressure and total temperature ratio, dry pressurized air at a pressure of 8.3 newtons per square centimeter and a temperature between 295 and 405 K was used for the primary flow, and gaseous nitrogen at a pressure between 8.3 and 11.6 newtons per square centimeter and a temperature between 195 and 295 K was used as vane coolant. The results of this investigation may be summarized as follows:

1. The overall thermodynamic efficiency increased with decreasing coolant-to-primary total pressure ratio and increasing primary-to-coolant total temperature ratio. At a coolant temperature and pressure ratio of 1.0, the percentage decrease in thermodynamic efficiency per percent coolant flow was 1.07.

2. A total pressure ratio contour plot at the vane exit survey plane showed that the ejection of coolant flow caused a considerably thicker and shallower wake compared to the plugged vane configuration.

3. A prediction method used to calculate the coolant flow fractions and overall primary and thermodynamic efficiencies for various coolant-to-primary total pressure ratios and primary-to-coolant total temperature ratios showed good agreement with the experimental results.

4. A comparison of the results from the subject investigation with those from a reference investigation having vanes with a larger aspect ratio showed that between a coolant-to-primary total pressure ratio of 1.0 and about 1.15, the level of efficiency for the subject vanes was lower and the penalty associated with the coolant flow was larger than that for the reference vanes. At a coolant temperature and pressure ratio of 1.0, the percentage decrease in thermodynamic efficiency per percent coolant flow was 0.57 for the reference configuration.

Lewis Research Center,
National Aeronautics and Space Administration,
and
U.S. Army Air Mobility R&D Laboratory,
Cleveland, Ohio, July 13, 1977,
505-04.

REFERENCES

1. Ewen, J. S.; Huber, F. W.; and Mitchell, J. P.: Investigation of the Aerodynamic Performance of Small Axial Turbines. ASME Paper 73-GT-3, April, 1973.

2. Rohlik, Harold E.; et al.: Secondary Flows and Boundary-Layer Accumulations in Turbine Nozzles. NACA Rept. 1168, 1954.

3. Haas, Jeffrey E.; and Kofskey, Milton G.: Effect of Coolant Flow Ejection on Aerodynamic Performance of Low-Aspect-Ratio Vanes. I - Performance with Coolant Ejection Holes Plugged. NASA TM X-3395, 1976.

4. Goldman, Louis J.: Cooled-Turbine Aerodynamic Performance Prediction from Reduced Primary to Coolant Total-Temperature-Ratio Results. NASA TN D-8312, 1976.

5. Goldman, Louis J.; and McLallin, Kerry L.: Cold-Air Annular-Cascade Investigation of Aerodynamic Performance of Cooled Turbine Vanes. I - Facility Description and Base (Solid) Vane Performance. NASA TM X-3006, 1974.

6. Whitney, Warren J.; Szanca, Edward M.; and Behning, Frank P.: Cold-Air Investigation of a Turbine with Stator-Blade Trailing-Edge Coolant Ejection. I - Overall Stator Performance. NASA TM X-1901, 1969.

7. Prust, Herman W., Jr.; Schum, Harold J.; and Szanca, Edward M.: Cold-Air Investigation of a Turbine with Transpiration-Cooled Stator Blades. I - Performance of Stator with Discrete Hold Blading. NASA TM X-2094, 1970.

8. Moffitt, Thomas P.; et al.: Summary of Cold-Air Tests of a Single-Stage Turbine with Various Cooling Techniques. NASA TM X-52968, 1971.

9. Stabe, Roy G.; and Dengler, Robert P.: Experimental Investigation of Aerodynamic Performance of Cooled Turbine Vanes at Gas-to-Coolant-Temperature Ratios Up to 2.75. NASA TM X-2733, 1973.

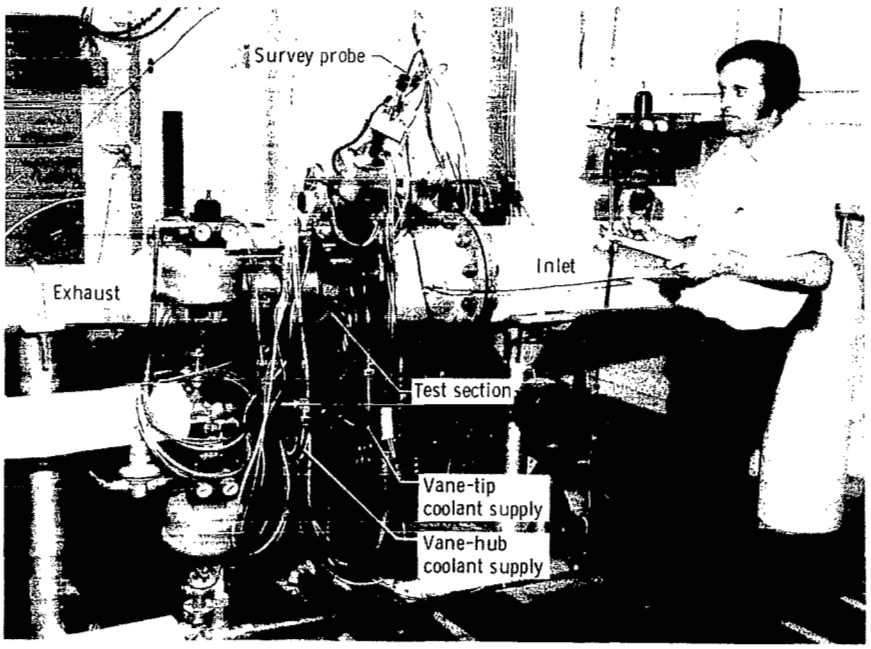

Figure 1. - Photograph of test facility.

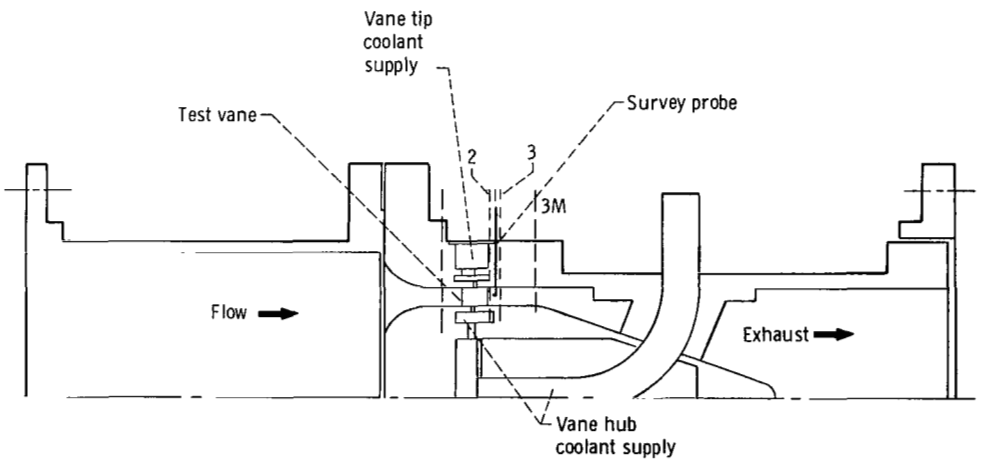

Figure 2. - Schematic cross-sectional view of stator vane cascade.

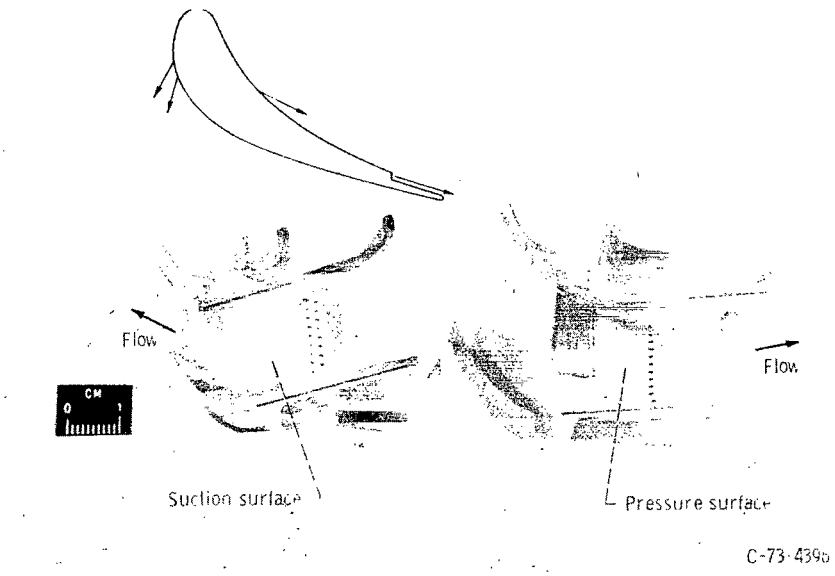

Figure 3. - Stator vane segments with coolant air ejection holes unplugged.

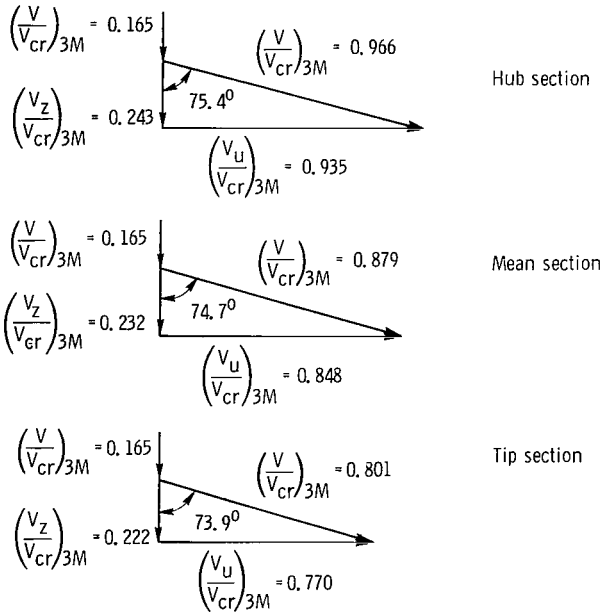

Figure 4. - Stator vane design velocity diagrams.

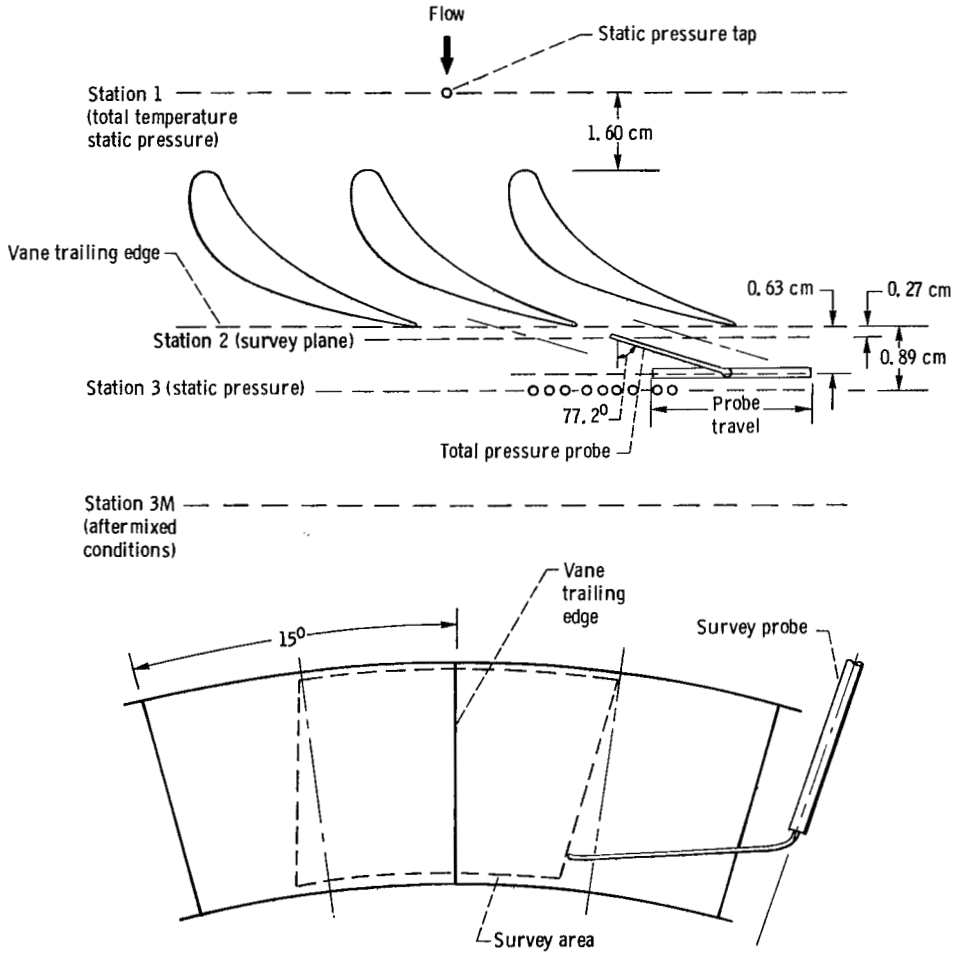

Figure 5. - Schematic of instrumentation for survey data.

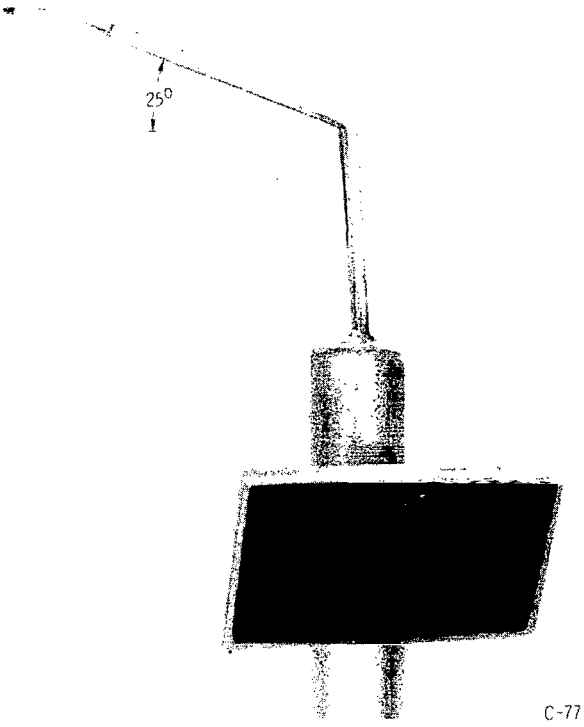

C-77-572

C-77-573

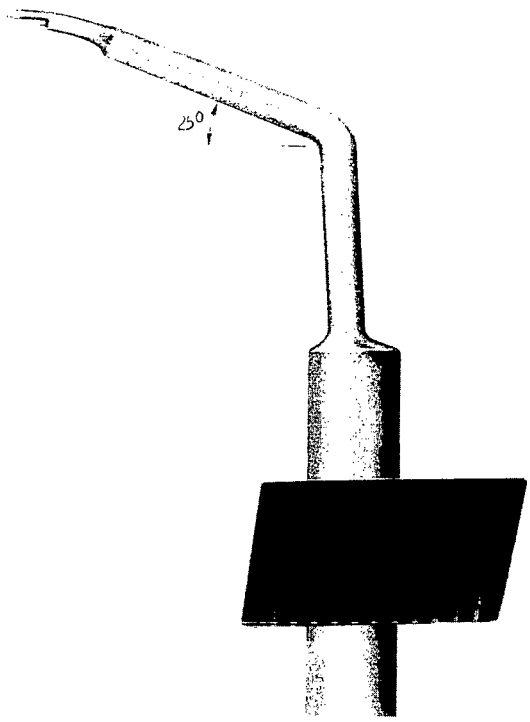

Figure 7. - Total pressure-total temperature probe.

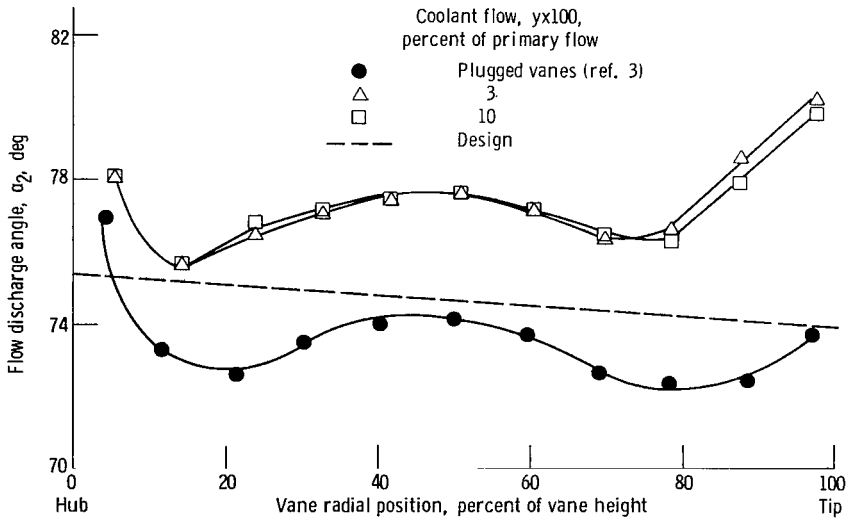

Figure 8. - Radial variation of flow discharge angle.

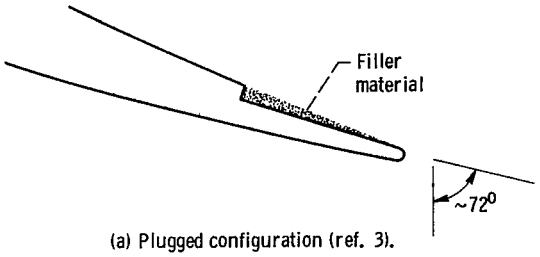

(a) Plugged configuration (ref. 3).

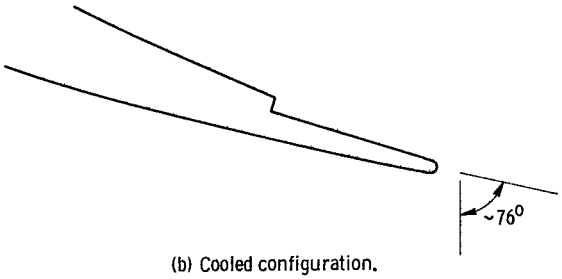

(b) Cooled configuration.

Figure 9. - Comparison of vane mean camber angles at trailing edge for plugged and cooled configurations.

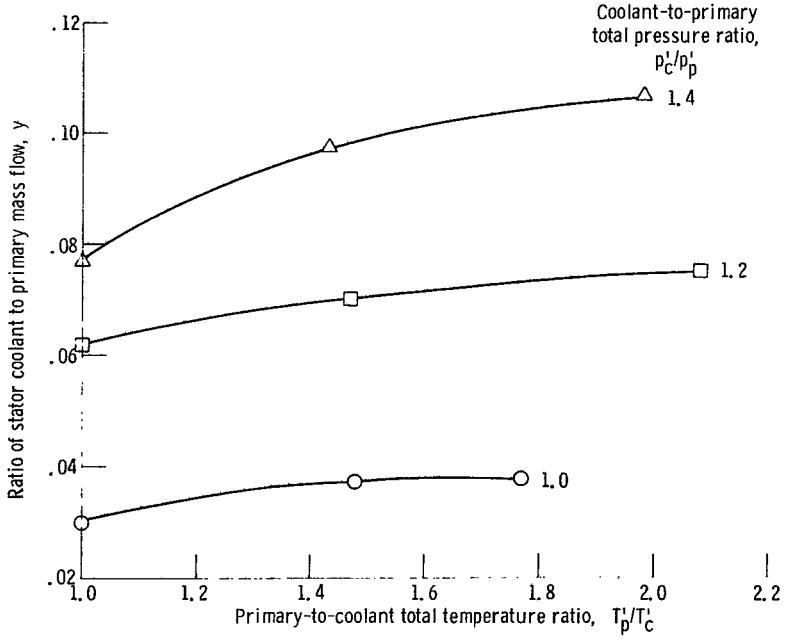

Figure 10. - Variation of coolant flow with coolant temperature and pressure ratio.

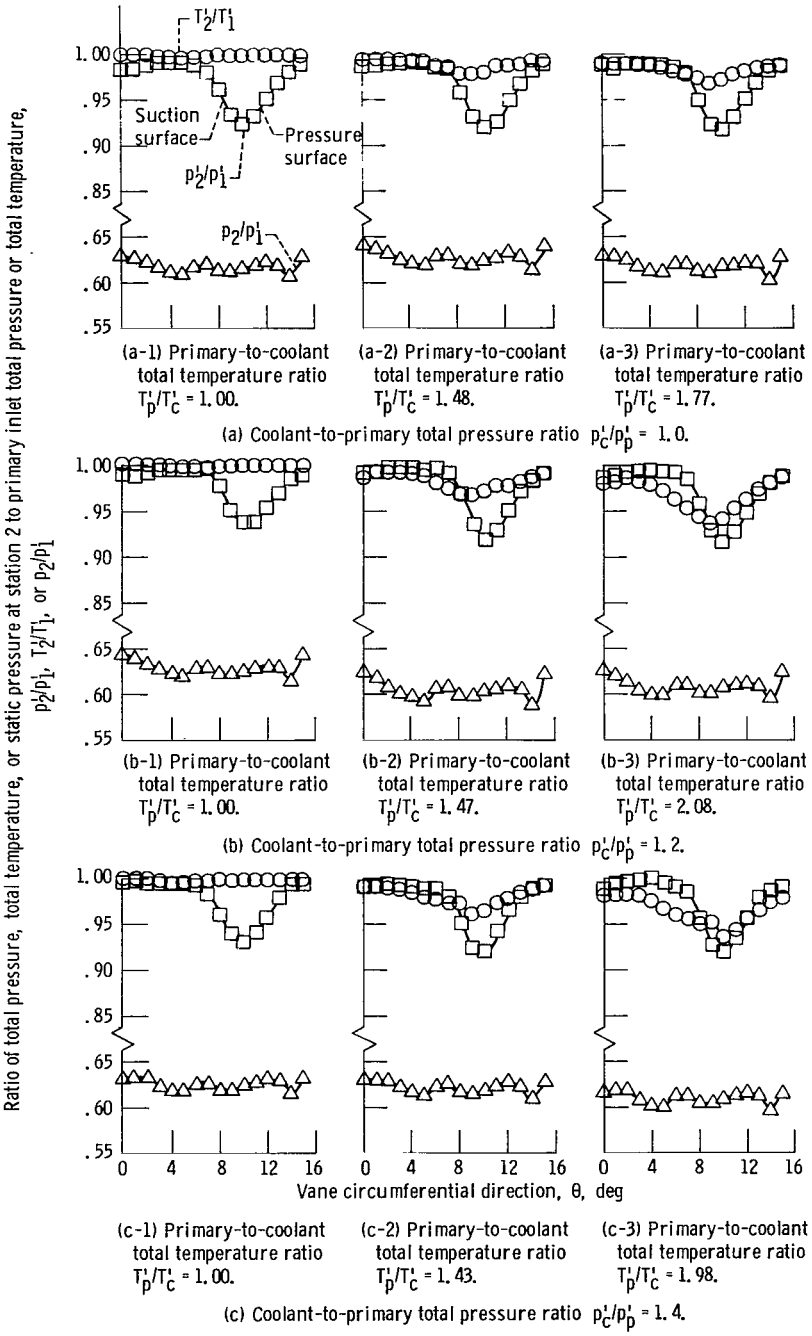

(a-1) Primary-to-coolant total temperature ratio $T_p'/T_c' = 1.00$.

(a-2) Primary-to-coolant total temperature ratio $T_p'/T_c' = 1.48$.

(a-3) Primary-to-coolant total temperature ratio $T_p'/T_c' = 1.77$.

(a) Coolant-to-primary total pressure ratio $p_c'/p_p' = 1.0$.

(b-1) Primary-to-coolant total temperature ratio $T_p'/T_c' = 1.00$.

(b-2) Primary-to-coolant total temperature ratio $T_p'/T_c' = 1.47$.

(b-3) Primary-to-coolant total temperature ratio $T_p'/T_c' = 2.08$.

(b) Coolant-to-primary total pressure ratio $p_c'/p_p' = 1.2$.

(c-1) Primary-to-coolant total temperature ratio $T_p'/T_c' = 1.00$.

(c-2) Primary-to-coolant total temperature ratio $T_p'/T_c' = 1.43$.

(c-3) Primary-to-coolant total temperature ratio $T_p'/T_c' = 1.98$.

(c) Coolant-to-primary total pressure ratio $p_c'/p_p' = 1.4$.

Figure 11. - Blade-to-blade midspan variation of total pressure, static pressure, and total temperature at station 2.

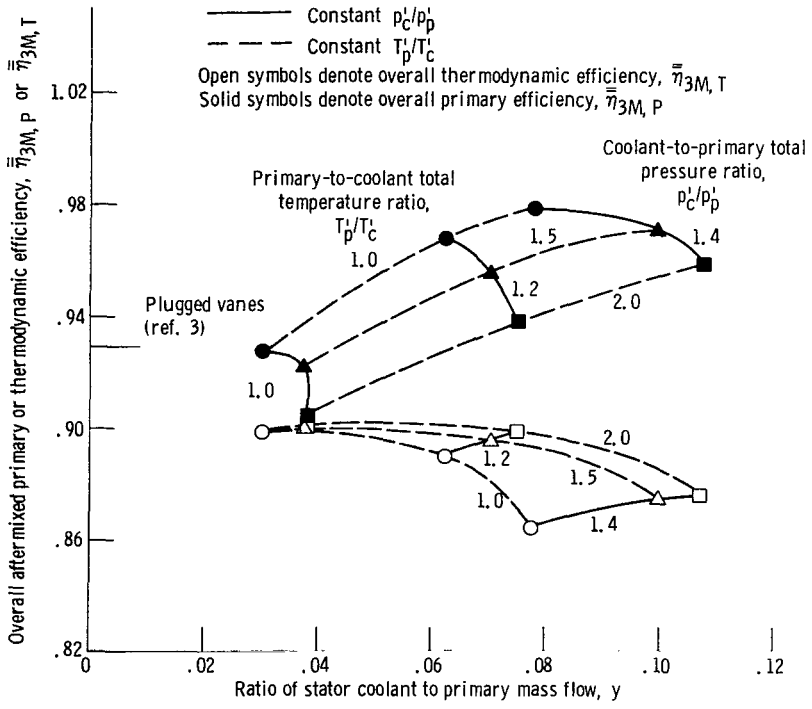

Figure 12. - Variation of overall primary and thermodynamic efficiency with coolant temperature and pressure ratio.

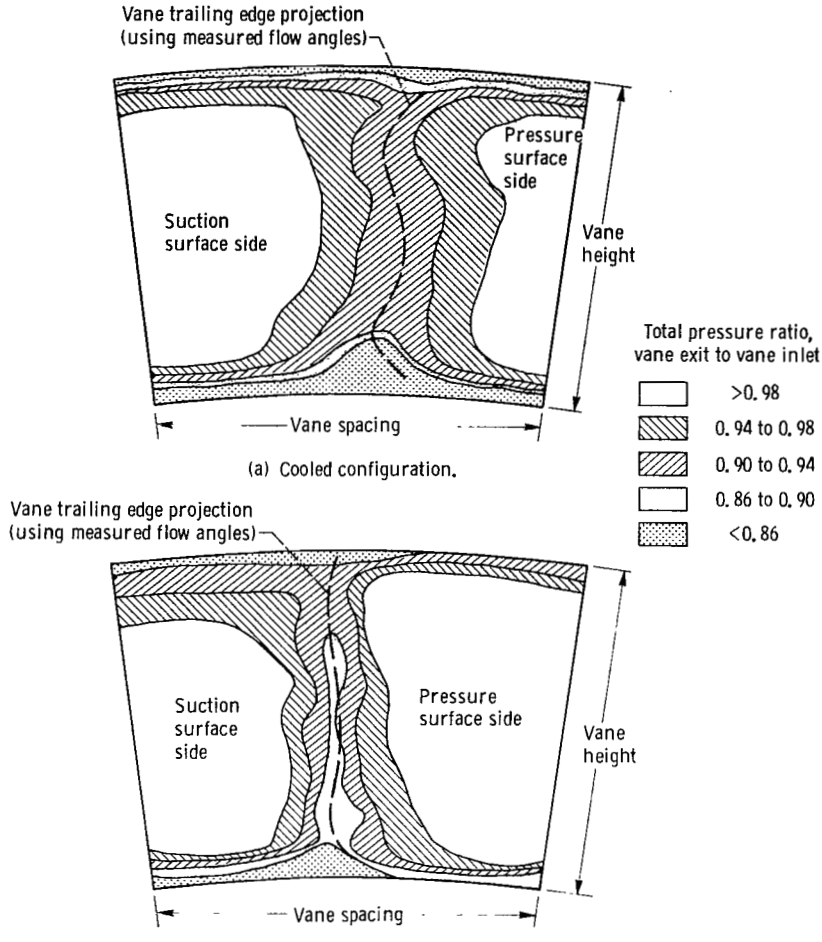

Figure 13. - Contours of total pressure at survey plane. Coolant-to-primary total pressure ratio $p'_c/p'_p = 1.4$; primary-to-coolant total temperature ratio $T'_p/T'_c = 1.98$.

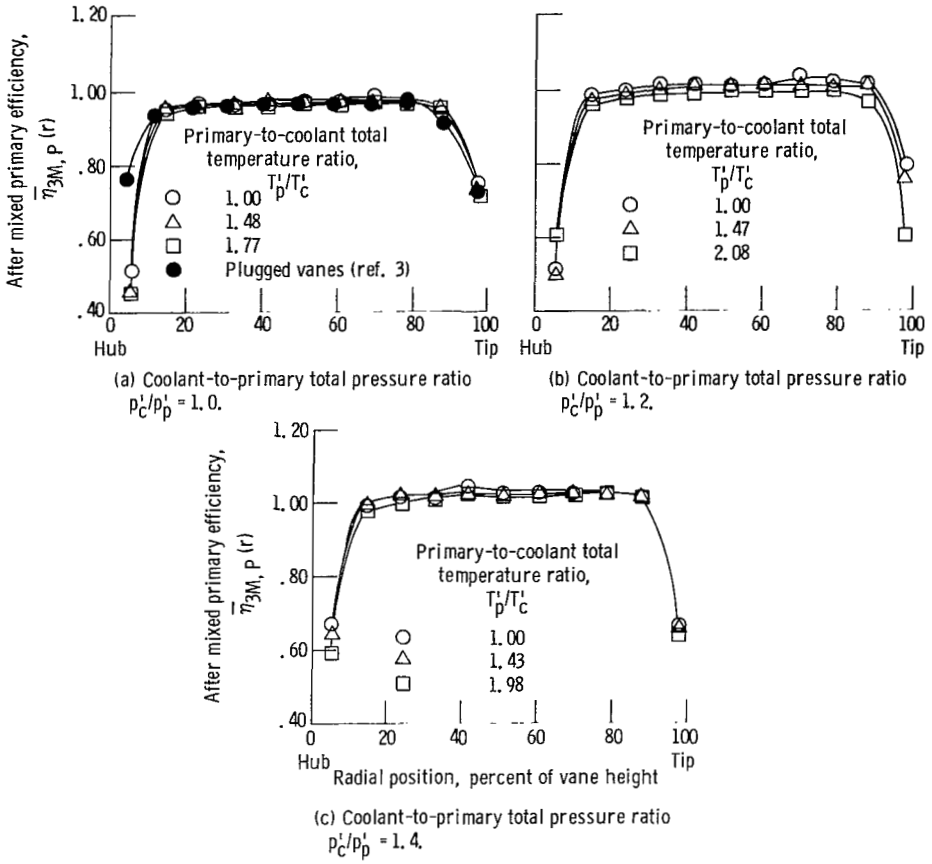

(a) Coolant-to-primary total pressure ratio $p'_c/p'_p = 1.0$.

(b) Coolant-to-primary total pressure ratio $p'_c/p'_p = 1.2$.

(c) Coolant-to-primary total pressure ratio $p'_c/p'_p = 1.4$.

Figure 14. - Radial variation of aftermixed primary efficiency with coolant temperature and pressure ratio.

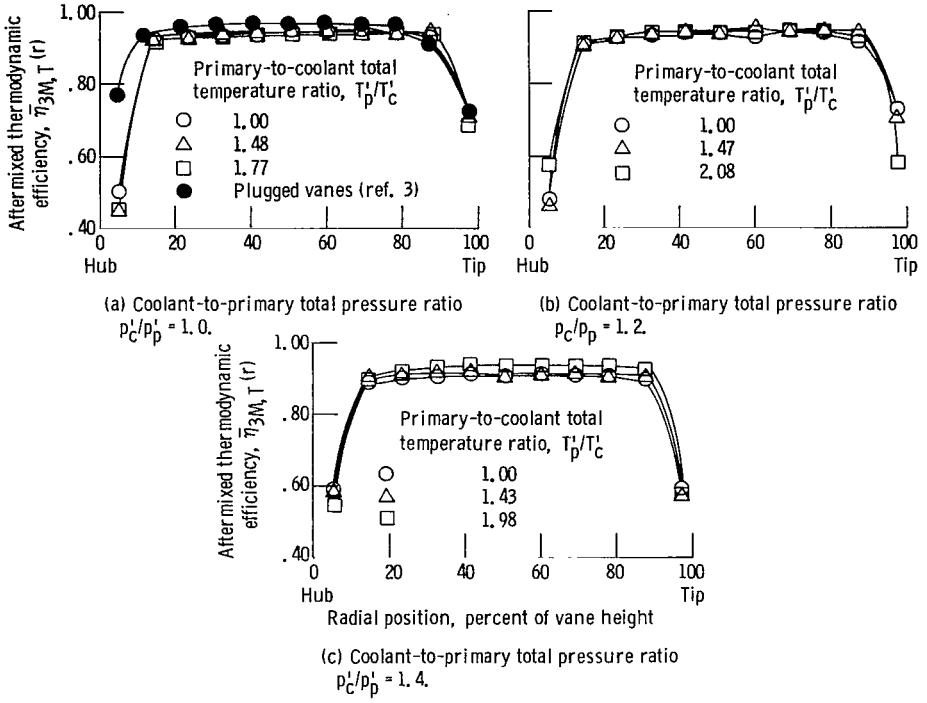

(a) Coolant-to-primary total pressure ratio $p'_c/p'_p = 1.0$.

(b) Coolant-to-primary total pressure ratio $p_c/p_p = 1.2$.

(c) Coolant-to-primary total pressure ratio $p'_c/p'_p = 1.4$.

Figure 15. - Radial variation of aftermixed thermodynamic efficiency with coolant temperature and pressure ratio.

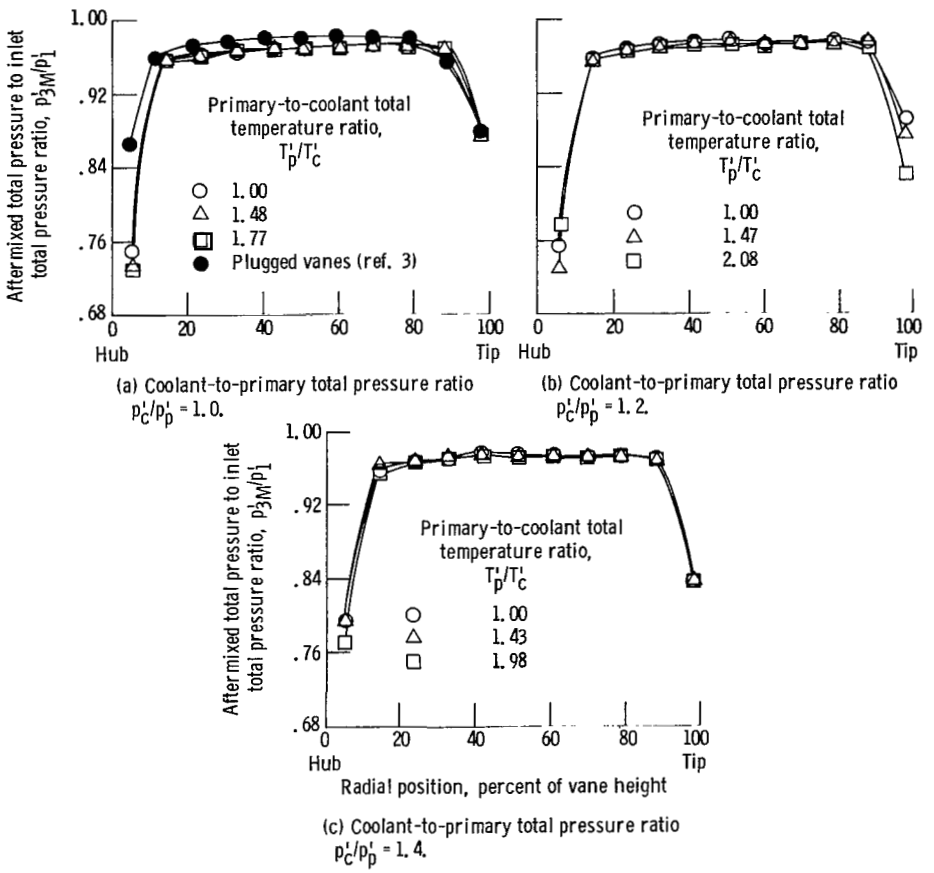

(a) Coolant-to-primary total pressure ratio $p'_c/p'_p = 1.0$.

(b) Coolant-to-primary total pressure ratio $p'_c/p'_p = 1.2$.

(c) Coolant-to-primary total pressure ratio $p'_c/p'_p = 1.4$.

Figure 16. - Radial variation of aftermixed total pressure ratio with coolant temperature and pressure ratio.

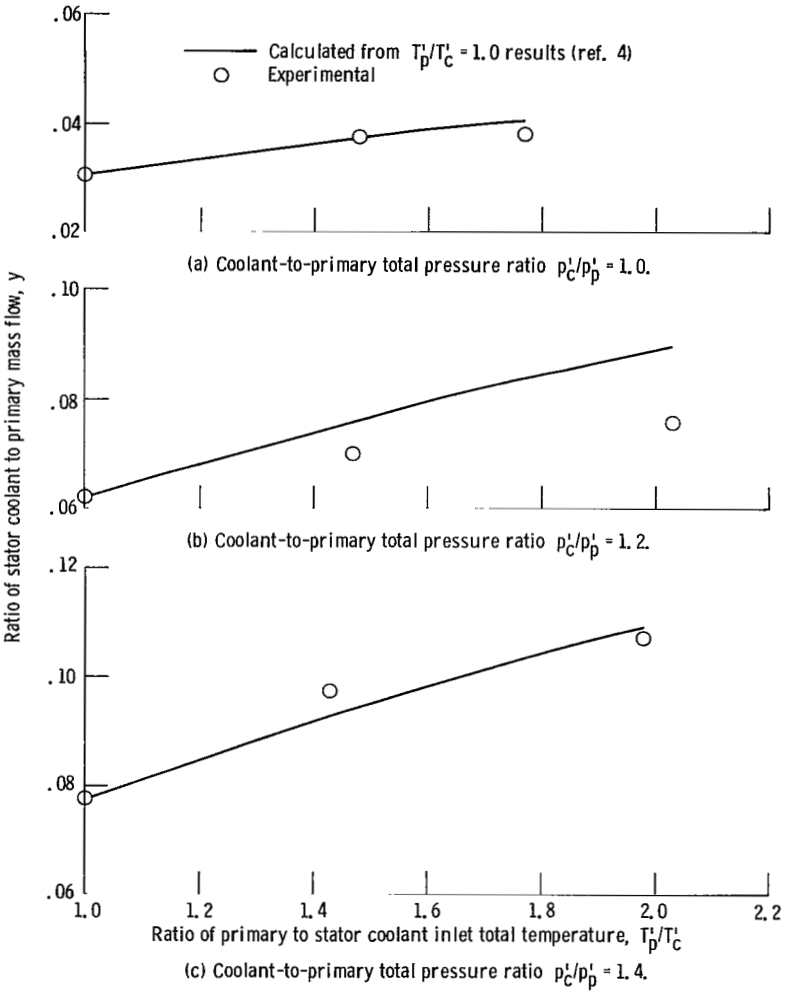

(a) Coolant-to-primary total pressure ratio $p_c'/p_p' = 1.0$.

(b) Coolant-to-primary total pressure ratio $p_c'/p_p' = 1.2$.

(c) Coolant-to-primary total pressure ratio $p_c'/p_p' = 1.4$.

Figure 17. - Comparison of calculated and measured coolant flow rate.

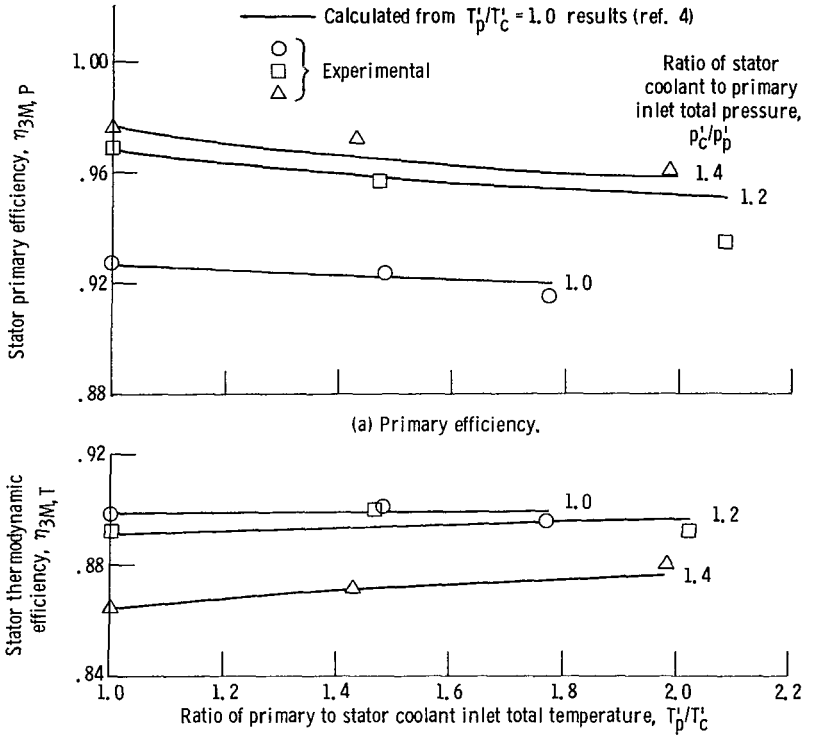

Figure 18. - Comparison of calculated and measured overall aftermixed primary and thermodynamic efficiencies.

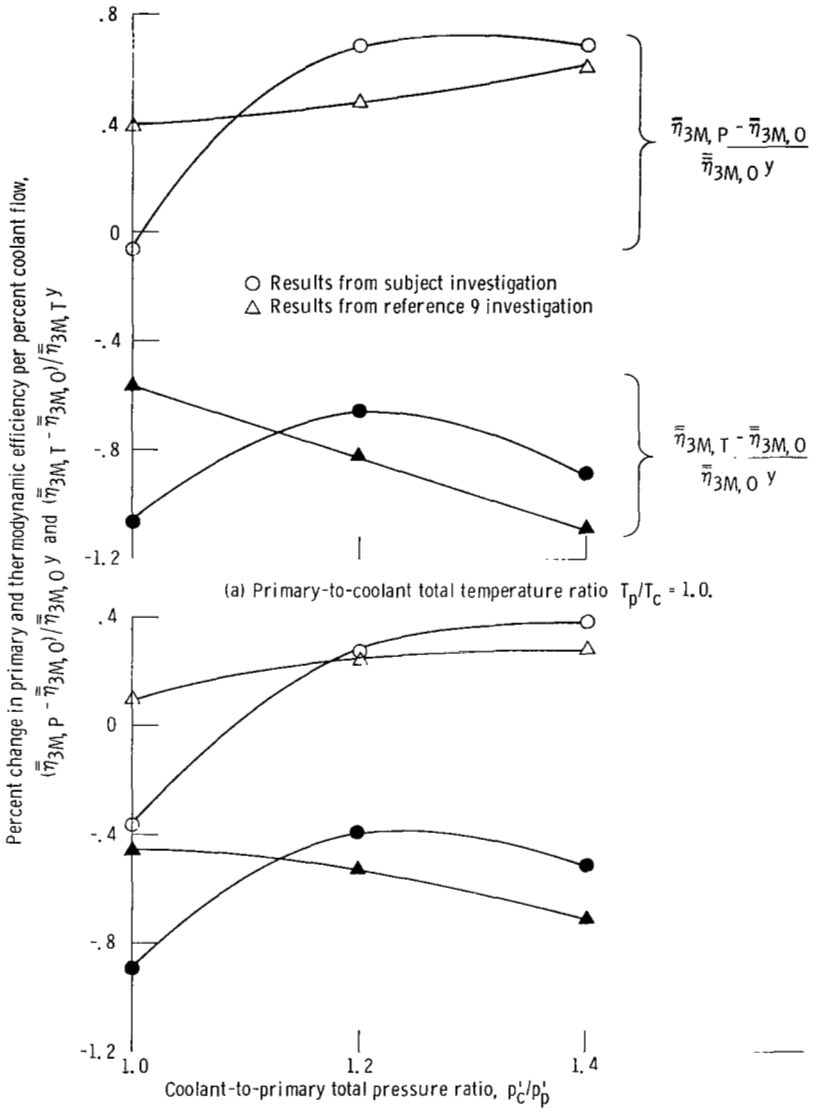

(a) Primary-to-coolant total temperature ratio $T_p/T_c = 1.0$.

(b) Primary-to-coolant total temperature ratio $T'_p/T'_c = 1.75$.

Figure 19. - Comparison of the experimental efficiencies for the subject vane configuration and the reference 9 vane configuration.

1. Report No.	2. Government Accession No.	3. Recipient's Catalog No.
NASA TP-1057		

4. Title and Subtitle: EFFECT OF COOLANT FLOW EJECTION ON AERODYNAMIC PERFORMANCE OF LOW-ASPECT-RATIO VANES. II - PERFORMANCE WITH COOLANT FLOW EJECTION AT TEMPERATURE RATIOS UP TO 2

5. Report Date: October 1977

6. Performing Organization Code:

7. Author(s): Jeffrey E. Haas and Milton G. Kofskey

8. Performing Organization Report No.: E-9213

9. Performing Organization Name and Address:
NASA Lewis Research Center and
U.S. Army Air Mobility R&D Laboratory
Cleveland, Ohio 44135

10. Work Unit No.: 505-04

11. Contract or Grant No.:

12. Sponsoring Agency Name and Address:
National Aeronautics and Space Administration
Washington, D.C. 20546

13. Type of Report and Period Covered: Technical Memorandum

14. Sponsoring Agency Code:

15 Supplementary Notes:

16 Abstract

The aerodynamic performance of a 0.5 aspect ratio turbine vane configuration with coolant flow ejection was experimentally determined in a full-annular cascade. The vanes were tested at a nominal mean-section ideal critical velocity ratio of 0.890 over a range of primary-to-coolant total temperature ratio from 1.0 to 2.08 and a range of coolant-to-primary total pressure ratio from 1.0 to 1.4. This corresponded to coolant flows from 3.0 to 10.7 percent of the primary flow. The variations in primary and thermodynamic efficiency and exit flow conditions with circumferential and radial position were obtained.

17. Key Words (Suggested by Author(s))	18 Distribution Statement
Aerodynamic performance Cooled turbine vanes	Unclassified - unlimited STAR Category 02

19 Security Classif (of this report)	20 Security Classif (of this page)	21 No of Pages	22 Price*
Unclassified	Unclassified	32	A03

* For sale by the National Technical Information Service Springfield Virginia 22161

NASA-Langley, 1977

DEPT OF THE AIR FORCE
AF WEAPONS LABORATORY
ATTN: TECHNICAL LIBRARY (SUL)
KIRTLAND AFB NM 87117